IRAM Newsletter

Number 24 November 24, 1995

Calendar

December 7-8th, 1995: IRAM User Meeting in Grenoble, France.

December 11-13th, 1995: ESO/IRAM/NFRA/OSO Worshop on Science with Large Millimeter Arrays, Garching, Germany.

March 4th, 1996: Deadline for the submission of observing proposals for the period May 15, 1996 to Nov. 15, 1996.

Contents

Invitation: IRAM User Meeting at Grenoble

December 7th and 8th, 1995

Preliminary Agenda

December 7th (morning)

CHAIRMAN : J.Martin Pintado

09:00-09:15	Opening of the meeting	M.Grewing
09:15-10:00	Status report on the 30m Telescope	W.Wild
10:00-10:15	Discussion	
10:15-10:45	Status report on the key project	E.Falgarone
10:45-11:00	Discussion	
11:00-11:15	Coffee Break	
11:15-11:35	Spectral-line on-the-fly observations with the 30m Telescope: Tests — Current Capabilities — Future plans	H.Ungerechts
11:35-11:45	Discussion	
11:45-12:05	Status Report on VLBI Observations	A.Greve,T.P.Krichbaum
12:05-12:15	Discussion	
12:15-12:30	Short spacings using the IRAM 30m Telescope	F.Viallefond
12:45-14:00	Lunch Break	

December 7th (afternoon)

CHAIRMAN : R.Wielebinski

14:00-14:45	Status report on the PdB Interferometer	S.Guilloteau
14:45-15:00	Discussion	
15:00-15:30	Future heterodyne receivers for the 30m and the PdB Telescopes	J.Lamb
15:30-15:40	Discussion	
15:40-16:00	Status of the heterodyne multibeam project	K.Schuster
16:00-16:15	Future backends	M.Torres
16:15-16:30	Coffee break	
16:30-17:00	Ongoing/Future bolometer developments for the 30m Telescope	
	Development work at the MPIfR	N.N.
	DIABOLO - A dual-channel photometer	J.-L.Puget
	Perspectives	B.Lazareff
17:00-17:15	Discussion	
17:15-17:45	Time Allocation Statistics and Discussion	M.Grewing
17:45-18:30	Options for IRAM's participation in future projects and General Discussion	
18:30-	Informal Reception at IRAM	

December 8th

CHAIRMAN : F.Viallefond

9:00–10:45	PdB interferometric survey of discs around T Tauri stars in the Taurus-Auriga cloud at 2.7mm	A.Dutrey
	Evolution of outflow activity around low-mass embedded young stellar objects	S.Bontemps
	Herbig-Haro jets. CO flows and CO bullets: The case of HH111	J.Cernicharo
	Density structure of protostellar envelopes at 1.3mm	F.Motte
	Low-mass star formation: Observations and non-LTE modelling	H.Wiesemeyer
10:45–11:00	Coffee break	
11:00–12:15	Recent results of cometary line observations	D.Despois
	The 12C/13C abundance in the far-outer Galaxy	J.Brand
	PdB observations of hot cores	R.Cesaroni
	Molecular gas dynamics at the center of spirals revisited: New high-resolution observations	S.Garcia-B.
	First mm-mapping of M87 at 89 GHz	D.Fraix-Burnet
12:15	End of the User Meeting	

30m Telescope

Second 3 mm SIS receiver available: first four receiver operation at Pico Veleta

A second 3 mm SIS receiver has been installed on October 18/19. This is the first time that four receivers (two 3 mm and two 1.3 mm receivers) can be used simultaneously at the 30m telescope. The 2 mm receiver can be used, as before, in combination with 3mm1 and 1.3 mm G1.

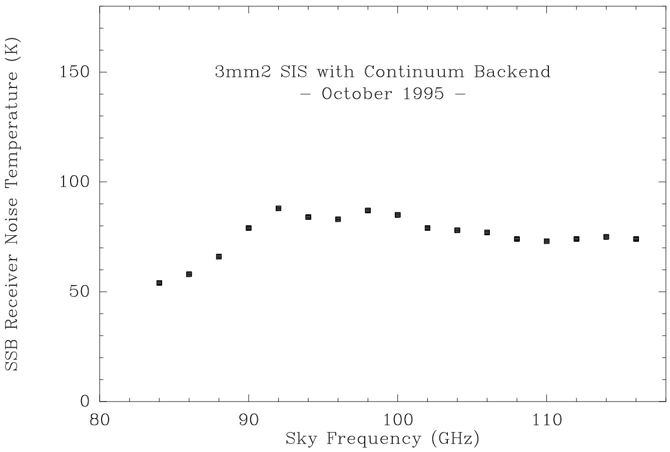

Figure 1: Single sideband receiver temperature of the newly installed second 3 mm SIS receiver (3mm2) at Pico Veleta. Temperatures were measured with the telescope calibration system and include optical losses and spillover. Image sideband rejection ranged from 25 dB to 40 dB.

The receiver construction was done mostly in Granada with components manufactured in Grenoble. Receiver temperatures (SSB) across the tuning band (82 - 116 GHz) are in the range 55 - 85 K (Figure 1). The receiver is tuned under remote control, and has very high sideband rejection (up to 40 dB). Laboratory measurements showed very good stability which seems to be reproduced at the telescope. No frequency switch test could be done so far.

Figure 2 shows the result of a pointing scan across Saturn with the two 3 mm receivers. Antenna temperatures and beam widths of the first ("old") 3 mm receiver (now called 3mm1) and the second (new) 3 mm receiver (called 3mm2) are almost identical. The relative alignment of the two receivers is better than 2″.

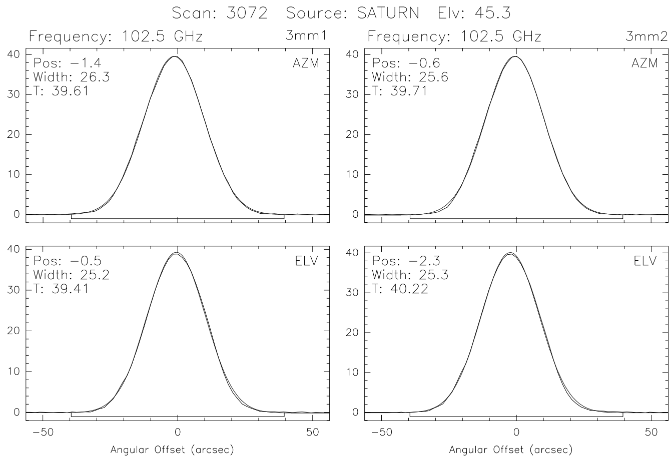

Figure 2: Result of a pointing cross scan on Saturn using both 3 mm receivers. Note the excellent agreement of antenna temperatures and beam widths between the first 3 mm receiver (left hand side) and the newly installed second 3 mm receiver (right hand side). The relative alignment of both receivers is better than 2″.

30m Manual available

A handbook for the 30m telescope, "The 30m Manual", is available now. This handbook has been written for both first time users and experienced users of the telescope. The manual does not intend to replace other, more detailed manuals (like the OBS manual, GAG software manuals etc.). It is rather a collection of useful information about the 30m telescope. Among other things, it describes antenna parameters, the receiver and backend system, data backup, and typical observing sessions. It also contains information about atmospheric opacities in the various frequency ranges, the pointing catalogue, and travel information to and from Granada.

Version 1.0 of the 30m Manual will be sent to the institutes and individuals who regularly receive the IRAM preprints. Updates of the manual will not be sent automatically in paper form. The latest version can be retrieved via WWW and Mosaic by connecting to the IRAM Grenoble home page (`http://iram.fr/`) and following the links, or via anonymous ftp. Connect through `ftp to iraux2.iram.fr` (or 193.48.252.22), username *anonymous*. Go to the directory `/dist/30m` and get the postscript file `manual.ps` (file size ~1.6 Mbyte). On a postscript printer you can print the file.

1 GHz bandwidth for the 1.3 mm G2 receiver

The 1.3 mm G2 receiver is now available with a 1 GHz bandwidth in combination with the 1 MHz filter banks. A new down converter and IF processor for the 1 MHz filter banks has been built and installed. The 230G2 receiver can be operated in two modes: narrow (512 MHz bandwidth) and wide (1 GHz bandwidth). The narrow mode is identical to the old mode of operation. The wide mode allows only the 1 MHz filter bank to be connected, no other backend can be connected at the same time to 230G2. This is due to a necessary shift of center frequency of the receiver. The mode is specified in the command
`RECEIVER 230G2 [`*options*`]`.
The default is narrow mode (512 MHz).

More flexible configurations of the 1 MHz filter banks possible

A new IF processor allows to use the 1 MHz filter banks in a more flexible way: the 1 MHz filter banks are now split into 4 parts of 256×1MHz channels each. Any combination (*e.g.* 4×256MHz = 1024 MHz, or 2×512MHz etc.) and any shift of the 4 subbanks relative to each other (in steps of 32 MHz) is possible. Each part can be connected to a different (or the same) receiver. Connecting the four parts in series provides a 1 GHz wide backend (at present only usable with 230G2). The distinction between "first" and "second" 1 MHz filter bank is not necessary any more. The previous OBS commands `1_1MHZ` and `2_1MHZ` are replaced by a single command `1MHZ`. The syntax is similar to the autocorrelator command.

Extended tuning range for the first 3 mm receiver (3mm1)

The tuning range of the 3mm1 receiver has been extended towards the lower end. Sky frequencies can now be tuned from 81 GHz to 116 GHz.

More flexible narrow band continuum pointing mode

The narrow band continuum pointing mode has been changed. It can be used with the 1 MHz filter bank *only* and provides selectable band widths from 2 MHz to 32 MHz in steps of 2 MHz. This allows to choose the band width for the signal according to the velocity width of the emission (of an SiO maser for example). The syntax to select this pointing mode is:
`CONTINUUM` *nnn* `SWITCH/RECEIVER` *rx*
where *nnn* is the selected band width in MHz plus 100 and can be between 102 and 132 (in steps of 2). 102 means a bandwidth of 2 MHz, 104 of 4 MHz etc.

The 100 kHz filter bank cannot be used for narrow band continuum pointing.

Winter conditions expected soon at Pico Veleta

The first snow at Pico Veleta is expected soon (and even hoped for by many people in Granada). After cancellation of the ski world championship in the Sierra Nevada in February 1995 (because of lack of snow), the skiing company is convinced that this winter we will see lots of snow (the world championship is now scheduled for February 1996). If we believe this, it could mean that during the transition period regular transport in time to the telescope may be difficult (as is the case every year), and during winter conditions the transport cannot be as flexible as during summer. We ask observers to take this into account when planning their trips to the 30m telescope, and allow for delay in the transport to and from the telescope. The following table gives the transport times when the ratrac is used (i.e. when the Sierra Nevada is covered by snow):

Transport to and from the 30m telescope: Winter schedule (typically Nov – May, depending on snow conditions).

	Departure from	
	Granada Office	Telescope
Monday	08:15	10:45
Tuesday	08:15	10:45 and 16:15
Wednesday	No transport *	No transport *
Thursday	10:00	15:00
Friday	08:15	10:45 and 16:15

* Person transport (morning hours) may be available after contact and agreement with IRAM Granada (Javier Lobato).

Wolfgang WILD

Interferometer

Project status

Most projects (including backups) from the May 15 to Nov 15 period have already been completed. Only the most extended configuration (B2) is missing.

Program Committee Recommendations

Observing proposals were discussed by the last program committee, for a scheduling period starting Nov 15, 1995, to May 15, 1996(see details on Table 1). A programs will be scheduled in priority. Further time, if it becomes available, will go to B programs, taking into account scientific merit, crowding in certain right ascension ranges and general aspects of balance. B proposals will only be started in case of available observing time. Special recommendations have also been made for some of the "A" and "B" projects: the authors will be contacted directly by IRAM.

Please note that because of our lack of specific experience and also because of scheduling constraints, 1.3mm and long baselines observations will be performed on a "best effort" basis, *without guarantee of result.* We remind you that B projects which have not been started are no longer automatically resubmitted: authors have to resubmit them explicitly.

Weather conditions on Plateau de Bure

Figure 3 shows the water vapor content measured on Plateau de Bure between Nov 5 and Nov 7 (the various curves correspond to the different antennas). Very low water vapor content (less than 0.7 mm) persisted when the outside temperature was about -12 degrees. With the upcoming of warmer air (about 0 degrees), the water vapor content increased to about 3 mm.

Water vapor content well below 2mm is expected to occur frequently in winter, since the mean outside temperature is -10 degrees.

Receivers and Antennas

The 3 mm and 1.3 mm receivers of all antennas have now been re-aligned to within $2''$, thereby removing the pending limitations on dual-frequency observations. Surface adjustments and optimization of the subreflector position have also been performed to improve the overall efficiency.

Control System

We had anticipated to replace the central computer, a VAX-3100 from DEC, by an HP workstation, in order to provide a possibility to perform *a posteriori* phase correction on short time scales. Software preparation of this major change has been progressing well, but unfortunately major hardware components are still missing. In order to avoid immobilizing the interferometer in winter time, we now have decided to keep the VAX-3100 for this winter. Limited software modifications will be made to gain most of the benefit from the total power phase compensation system.

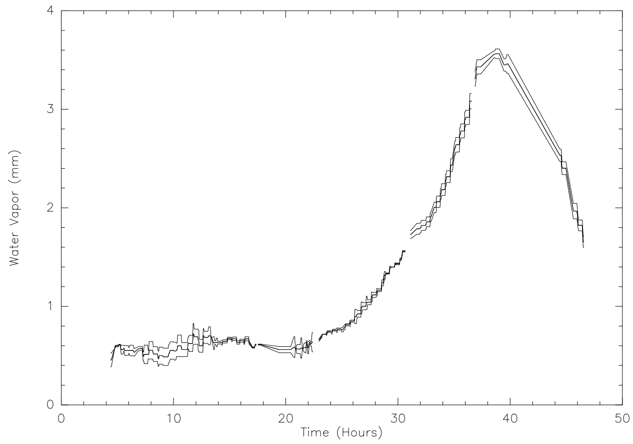

Figure 3: Water vapor content measured on Plateau de Bure between Nov 5 and Nov 7 (see text)

.

New configurations: Erratum

A slight mistake occurred in the table presenting the new configurations. The standard set includes 4 basic arrays, built upon a primary set of 8 4-antenna configurations.

Available configurations:

Conf.	AB	BC	CD	DD	Stations
A1	o				W27–W20–N29–E23
A2	o				W23–E04–N29–E24
B1		o			E24–E16–N11–N17
B2	o	o			W12–W09–E24–N20
C1	o	o	o		W20–W05–N09–N17
C2		o	o		W09–E10–N03–N15
D1			o	o	W05–W00–E03–N05
D2				o	W10–W01–E03–N09

230 GHz OBSERVATIONS ON PLATEAU DE BURE

Figure 4 is a result of observations at 230 GHz obtained on Nov 9, 1995. The array was in the most compact configuration (baselines from 24 to 64 meters), which already gives about 3″ resolution at the CO J=2-1 frequency. The figure shows images of the integrated intensity of the CO J=2-1 line, of the velocity field and of the line width of a proto-planetary disk around the T Tauri star GM Aur. The integrated spectrum is also shown. The data were obtained in snapshot mode (4 sources were observed during the same transit), so that the total integration time on source is less than 1.5 hours.

Keplerian rotation had been previously detected by aperture synthesis observations of ^{13}CO J =2-1 performed at OVRO (Koerner, Sargent & Beckwith 1993, Icarus 106, 2), with an angular resolution of 6″ by 3.5″. Despite the very short integration time, the Plateau de Bure data significantly improve the angular resolution and unambiguously confirm the Keplerian rotation.

Stéphane GUILLOTEAU

Atmospheric Phase Correction: from random phase down to 20 degree r.m.s. at 230 GHz

We have continued experimenting with the atmospheric phase compensation under various atmospheric conditions.

At the beginning of October, an analog/digital converter in the detector chain was found to dominate the noise of the total power signal. This was limiting the overall relative stability of the detection system to about 10^{-3}, thereby limiting the accuracy of the phase compensation to about 20-30 degrees rms in the 84-116 GHz band. Proper electronic grounding of the A/D converter has reduced its noise contribution by a factor 6, and the stability of the complete total power acquisition chain is now about 2 10^{-4}.

As a consequence, the rms of the corrected phase has been improved sufficiently to be of interest in the 210-248 GHz band. An example is given in Fig. 5, which shows a sequence observed on October 21st, after the passage of clouds, while the phase stabilized over a time interval of about 1.5 hours for a baseline of 176 m (the correction is independent of baseline length). Opacity was low, with a total amount of precipitable water around 3 mm.

The time resolution of the correction is one second, and it is exclusively based on the optical path predicted by the atmospheric model (M.Bremer & J.Cernicharo) from the calibrated total power. Phase noise histograms have been calculated to illustrate the effect of the correction. The scan based distributions peak in the $5-10°$ and $20-25°$ rms bins for 91.2 and 230.5 GHz, respectively.

The observed phase at 1.3mm moves too fast to be continuously traced; the atmospheric phase predicted from the total power fluctuations has indeed an r.m.s. of 196°. For an integration time of one minute, the gain in coherence of the 230 GHz continuum signal is spectacular.

Implementation of the phase correction software in the CLIC calibration program is under way. A full correction, with phase continuity from one source to another, is not possible because of slight, but significant, receiver gain variations for large telescope motions in elevation. Accordingly, the phase correction will be made with a zero mean. This can be done *a posteriori* for the continuum data which is sampled every second. This is not possible for the spectral line data which have an averaging interval of 1 or 2 minutes. Since the correction breaks down in the presence of clouds, we are currently working on a scheme which will provide both corrected and uncorrected spectral line data in real time.

Michael BREMER, Stéphane GUILLOTEAU,
Robert LUCAS

Table 1: Plateau de Bure: project status A: Accepted, B: Backup if available time, C: Rejected.

Project	Rate	Project	Rate	Project	Rate	Project	Rate	Project	Rate
F018	C	F022	C	F029	B	F030	A	F031	C
F032	B	F033	B	F034	B	F035	A	F036	C
F037	C	F038	A	F039	C	F040	C	F041	B
F042	B	F043	B	F044	A	F045	C	F046	A
F047	B	F048	C	F049	A	F050	A	F051	A
F052	B	F053	C	F054	A	F055	A	F056	A
F057	C	F058	A	F059	C	F060	B	F061	A
F062	A	F063	C	F064	A	F065	A	F066	C
F067	C	F068	A	F069	C	F070	C	F071	C
F072	C	F073	A	F074	B	F075	B	F076	C
F077	B	F078	A	F079	A	F080	C	F081	A
F082	A	F083	A	F084	B	F085	C	F086	A
F087	A	F088	C	F089	A	F090	C	F091	C
F092	C	F093	C	F094	C	F095	C	F096	B
F097	B	F098	A	F099	C	F100	C	F101	C
F102	C	F013	A						

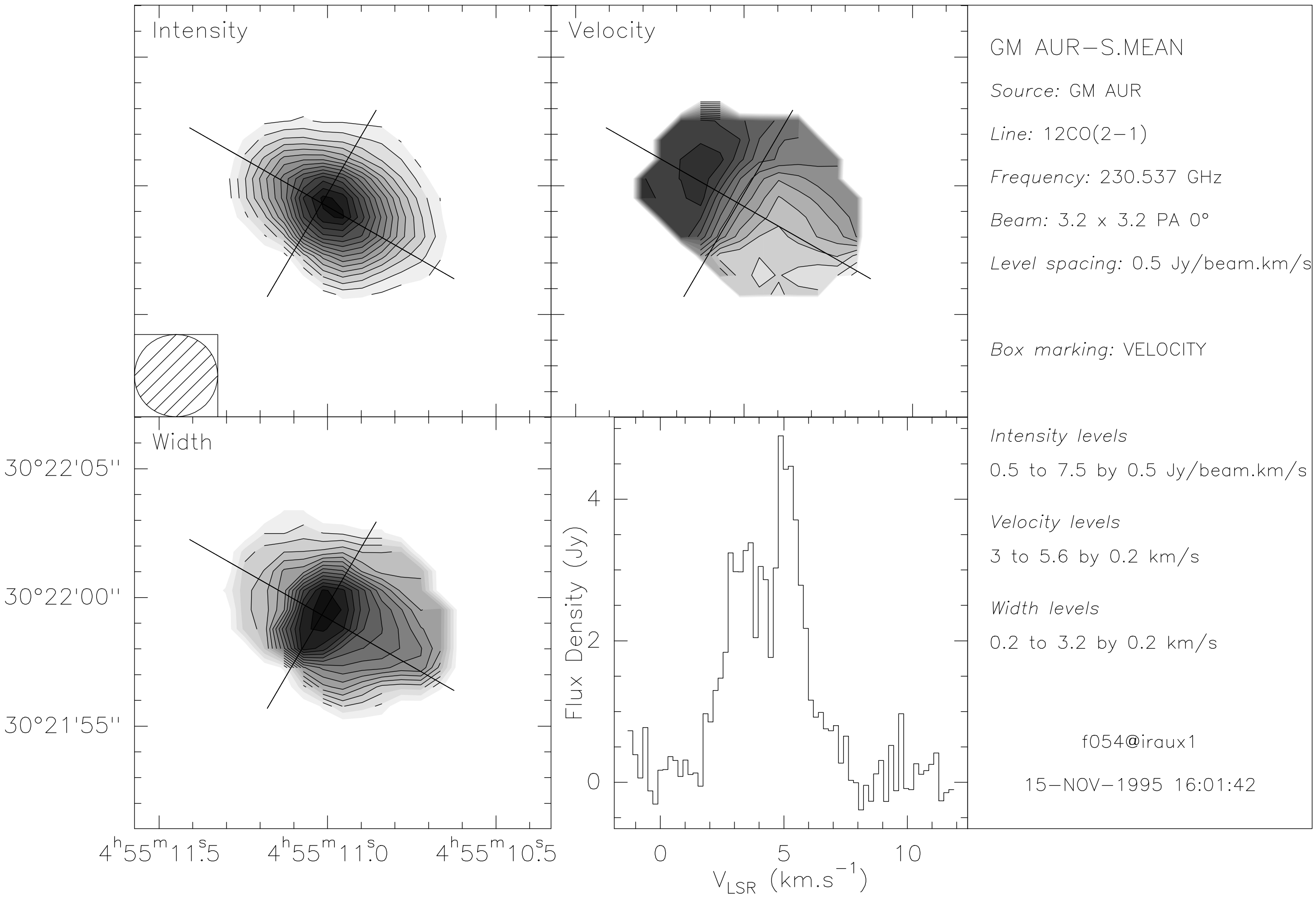

Figure 4: The proto-planetary disk around the T Tauri star GM Aur, observed with the Plateau de Bure interferometer on Nov 9, 1995 (1.5 hours of integration).

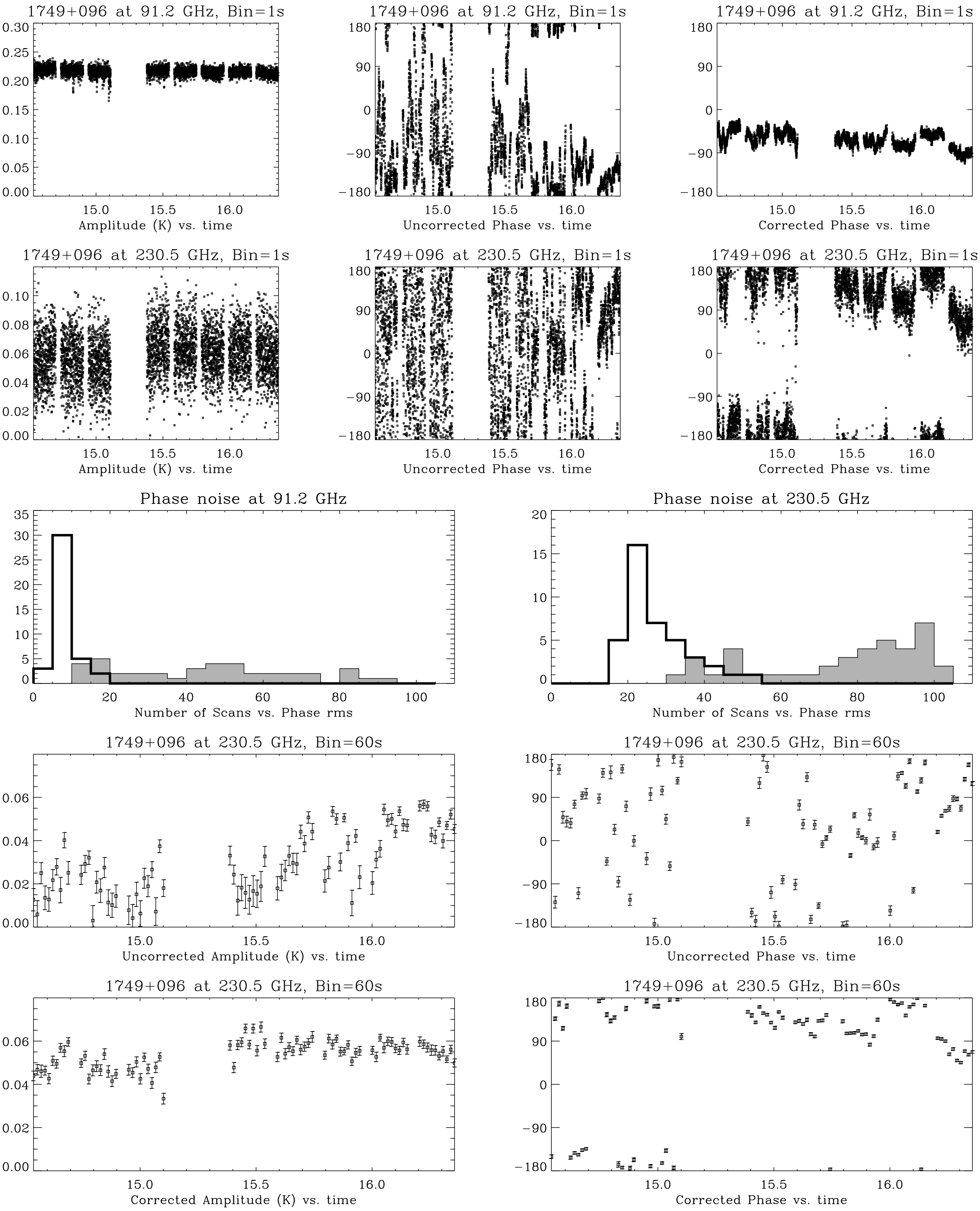

Figure 5: Model based phase correction at 91.2 and 230.5 GHz on October 21, baseline 176 m. *First two rows*: Amplitude, uncorrected and corrected phases for 91.2 and 230.5 GHz, respectively. *Third row*: Phase noise histograms of uncorrected phase (shaded) and corrected phase (thick line). One scan corresponds to 120 s of integration. *Last two rows*: amplitude and phase at 230.5 GHz have been vector-averaged over time bins of one minute. The bars mark the $\pm 1\sigma$ error of the average.

Report on Recent Observations

First Observations of Comet Hale-Bopp at the IRAM 30-m telescope

Report by: N. Biver([1]), D. Bockelée-Morvan([1]), P. Colom([1]), J. Crovisier([1]), D. Despois([2]), L. Jorda([1]), R. Moreno([3]), G. Paubert([3]), H. Rauer([1])
([1])Observatoire de Paris-Meudon
([2])Observatoire de Bordeaux
([3])IRAM (Granada)

When comet C/1995 O1 Hale-Bopp was discovered in late July at 7 AU from the Sun, it was already very bright: its magnitude was $m_v = 10.5$, which is about *250 times brighter* than comet Halley at the same heliocentric distance. Comet Hale-Bopp is a long-period comet, with a period of about 3000 years. It will reach perihelion on April 1, 1997 at 0.91 AU from the Sun and, although predictions of cometary evolution are highly unreliable, it might be at that time a very bright object, with possibly a negative magnitude. We could then have an unprecedented opportunity to investigate a very bright comet with modern instrumentation.

Comet Hale-Bopp is already an interesting object worth of detailed studies. Its coma shows rapidly evolving dust jets. The reason for this activity cannot be sublimation of water — which is the driver of cometary activity at small heliocentric distances — because it is inefficient at this distance.

Thanks to the IRAM staff and to observers who accepted last-minute changes to their observing schedule, observations of comet Hale-Bopp could take place as early as mid-August. We searched for volatile species in the coma. The CO $J(2-1)$ line was already marginally detected on Aug. 16 and 23. It was then confidently detected on Sept. 20 and 21 (Rauer *et al.* 1995, *IAU Circ.* No 6236) and observed at several subsequent periods. The same line was also independently detected at the JCMT (Matthews *et al.* 1995, *IAU Circ.* No 6234).

This CO spectrum resembles the one observed in another exceptional object, the short-period comet P/Schwassmann-Wachmann 1, which harbours gaseous activity although located beyond Jupiter on a nearly circular orbit (Crovisier *et al.* 1995, *Icarus* **115**, 213; also *IRAM Newsletter* No. 19). The line is blue shifted by 0.4 km s^{-1}, which indicates outgassing from the day-side of the nucleus. This anisotropic outgassing can be related to the dust jets seen in the visible images of the comet. Assumming a CO rotational temperature of 10 K — as was retrieved from observations of the $J(1-0)$ and $(2-1)$ lines in P/Schwassmann-Wachmann 1 — the CO production rate ranges between 1.3 and 4.2×10^{28} molec. s^{-1} (on the order of one ton per second), with indications of time variations, for our observations between Aug. 16 and Oct 22, 1995.

Although important, this CO production may not be sufficient to explain the huge dust production of this comet observed in the visible. We also searched for other volatiles: HCN, H_2CO, CH_3OH, which have sublimation temperatures between those of CO and H_2O. The search was negative, with upper limits corresponding to a few percent the production rate of CO.

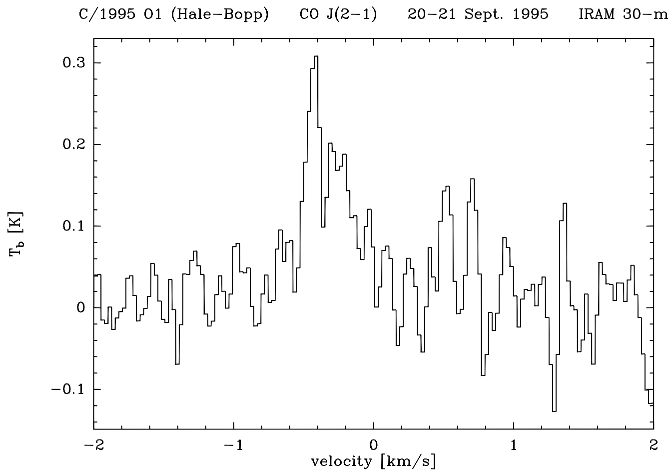

Figure 6: The CO $J(2-1)$ line observed in comet Hale-Bopp, average of September 20-21, 1995.

An open question is whether the activity of comet Hale-Bopp is due to the sublimation of carbon monoxide ice, or triggered by the amorphous-to-crystalline water ice transition, an exothermic process which induces the release of trapped volatiles. This would have different implications on the physical state of cometary ices and on their formation scenarios.

We plan to monitor the CO production of this comet and to watch for the onset of sublimation of other species as the comet approaches the Sun. Very sensitive spectral observations could be undertaken at IRAM in one year if this comet becomes indeed very bright. They would allow us to investigate the composition of the cometary ices and to obtain clues to their outgassing processes.

Scientific Results

Dust and Gas Distribution around T Tauri stars in Taurus-Auriga. I. Interferometric 2.7mm continuum and ^{13}CO J=1-0 observations

A.Dutrey ([1]), S.Guilloteau ([1]), G.Duvert ([2]), L.Prato ([3]), M.Simon ([3]), K.Schuster ([1]), F.Ménard ([2])
([1])Institut de Radio Astronomie Millimétrique, 300 Rue de la Piscine, F-38406 Saint Martin d'Hères, France
([2])Laboratoire d'Astrophysique de Grenoble, B.P. 53, F-38041 Grenoble Cedex 9, France
([3])Astronomy Program, State Univ. of New York, Stony Brook, NY 11794-2100, U.S.A.

Abstract: We present new ^{13}CO $J = 1 \rightarrow 0$ and 2.7 mm continuum interferometric observations of 33 young star systems located in Taurus-Auriga. Our goal was to compare the distribution, and hence the evolution, of the circumstellar material around young star singles and binaries. The sample included 2 triples, 16 binaries, 14 singles, and one object of unknown multiplicity.

We detected 2.7 mm continuum emission in 12 systems at S/N > 5 and have probable detections for another 5. V 773 Tau, a weak emission line binary system, is remarkable in that its 2.7 mm continuum decreased from $\sim$ 30 mJy to $\sim$ 0 mJy in less than six months. We find that the singles are, on average, stronger 2.7 continuum sources than the multiples, consistent with Osterloh & Beckwith's (1995) finding at 1.3 mm. Significant estimates of the sizes have been obtained for 8 singles. They imply large (R > 150 AU) disks, with relatively flat density distribution (emissivity flatter than $r^{-1.5}$). The spectral energy distributions in the millimeter range can be fitted using a dust emissivity law $K_\nu \propto \nu^\beta$ with value of β in the range 0.5 to 1.

Only DG Tau, Haro 6-5b and UY Aur have detectable ^{13}CO $J = 1 \rightarrow 0$ emission. ^{13}CO emission, but no 2.7 mm continuum, is also found in the LkHα 332 region and near FS Tau; however, it does not appear to be associated with the known stars. Interpreting the observational results in terms of the circumstellar disk scenario, we find that, in all cases, disk masses derived from the dust emission at 2.7 mm are more than a factor of about 20 larger than the masses derived from the ^{13}CO $J = 1 \rightarrow 0$ upper limit.

To appear in A&A main journal.
The full preprint is available as a postscript file on the WWW:
`http://iram.fr/papers/papers.html` *or by an anonymous ftp at:*
`iram.fr (/dist/pub/papers/e021.ps.Z).`

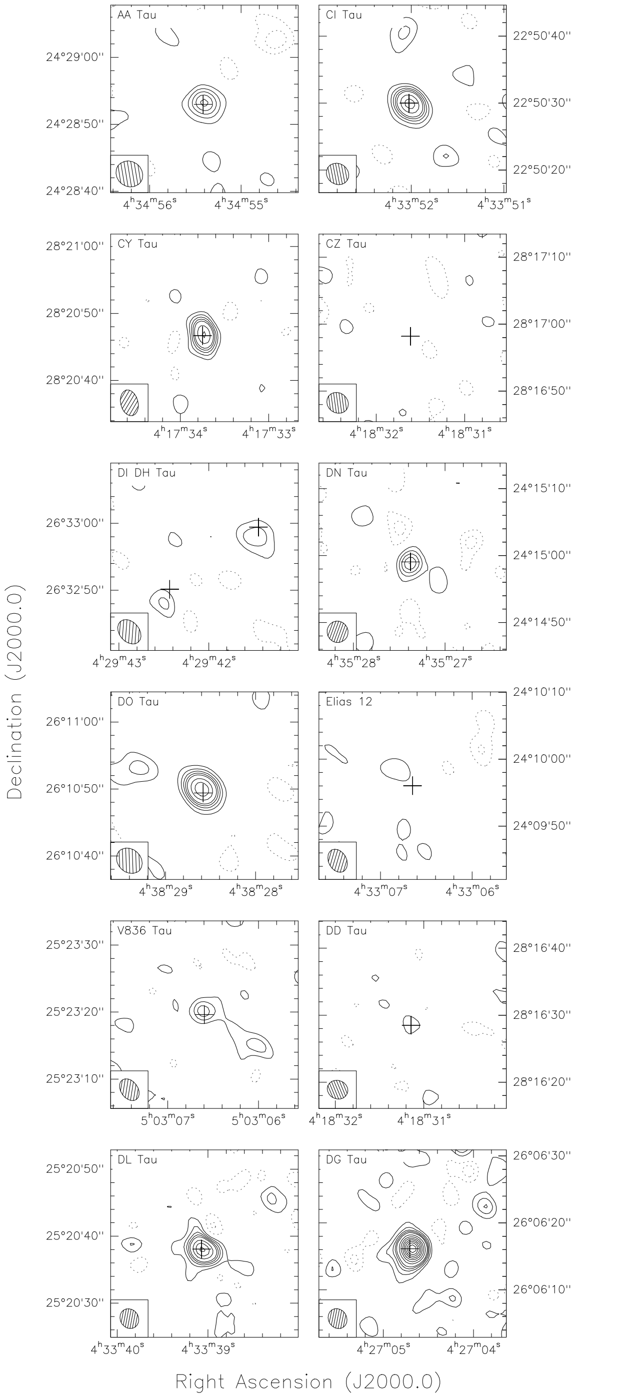

Figure 7: Continuum images of the observed stars. Contour steps are -4, -2, 2, 4, 6, 8 and then 10 to 50 by 5 mJy/beam. The name of the source is indicated in upper left corner, and the beam size in lower left. The crosses indicate the nominal position of the stars from HBC. Coordinates are in the J2000 system. Positions have been corrected for proper motions according to measurements by Jones and Herbig (1979) and Hartmann et al. (1991).

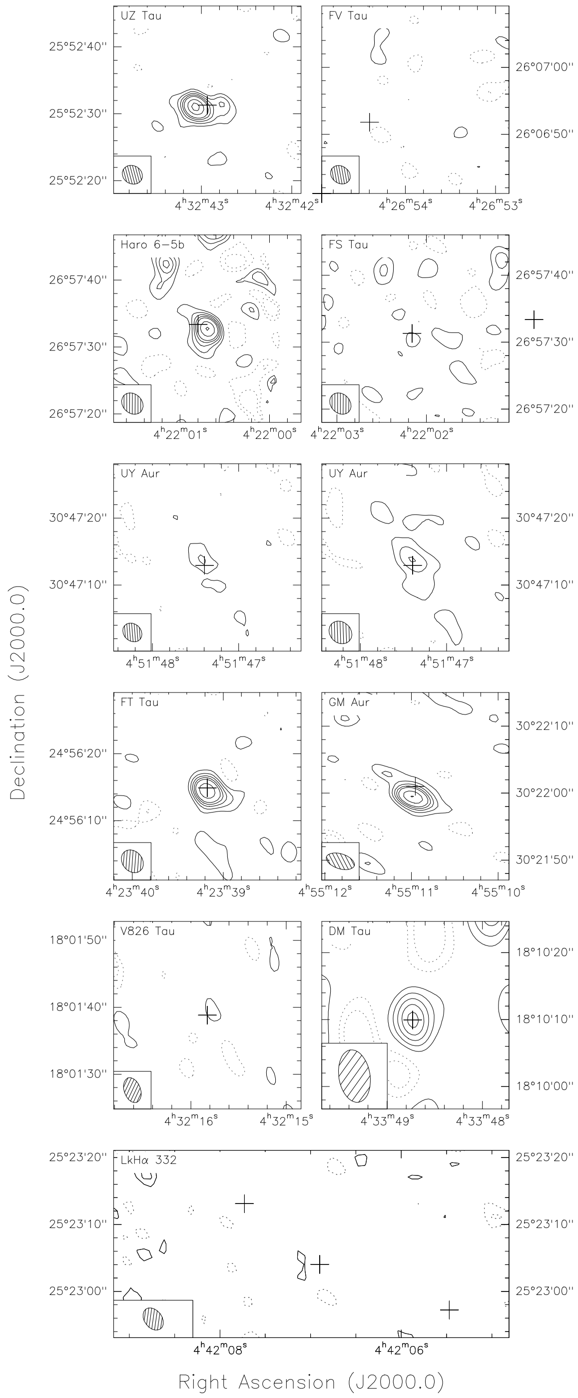

Figure 8: Continuum images of the observed stars (cont.). The upper limits for IW Tau, IS Tau, GH Tau, GK Tau and LkCa 3 (not shown here) were obtained with a beam similar to that of DM Tau. For UY Aur, we show two maps, one obtained at full resolution (left), the other (right) done with a 150-m taper. Since Haro 6-5b is displaced from the pointing center FS Tau, the map has been corrected from the primary beam attenuation. The S/N in this map decreases towards the north-west of the map, and contours to the north and north-west of Haro 6-5b are noise peaks. Note that GM Aur position has not been corrected for proper motion.

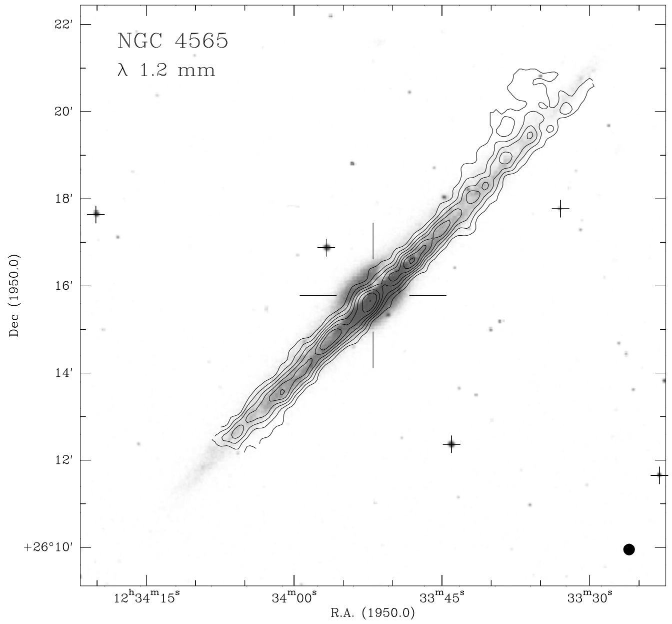

Figure 9: The λ 1.2 mm continuum emission, smoothed to an angular resolution of 20″ and superimposed on a optical photograph of NGC 4565 (Lick Observatory). The contour levels are 3.0 (3σ), 6.0, 9.0,... 21 mJy/20″ beam. The noise level increases by about 30% towards the outer parts of the map. Note the warp of the continuum contours to the NW.

Cold dust and molecular line emission in NGC 4565

N. Neininger([1,3]), M. Guélin ([1]), S. García-Burillo([2]), R. Zylka([3]), R. Wielebinski([3])
([1])Institut de Radioastronomie Millimétrique, 300, rue de la Piscine F-38406 St. Martin d'Hères, France
([2])Centro Astronómico de Yebes, IGN, E-19080 Guadalajara, Spain
([3]) Max-Planck-Institut für Radioastronomie, Auf dem Hügel 69, D-53121 Bonn, Germany

Abstract: Using the IRAM 30-m telescope, we have mapped the λ 1.2 mm continuum emission and the ^{12}CO J= 1→0 and 2→1 line emissions in the edge-on spiral galaxy NGC 4565. We selected NGC 4565 because it is strong in the HI line, but weak in CO, contrary to the galaxies mapped so far at 1.2 mm.

The CO emission in NGC 4565 resembles that in the Milky Way. It shows a compact central source surrounded by a 'molecular ring'. The molecular ring peaks between 1′ and 1.5′ from the center ($3-5$ kpc) and has an outer radius of $\simeq 3'$. It is twice smaller than the broad 'plateau' observed in HI and shows narrow structures which could be spiral arms.

The λ 1.2 mm continuum follows CO near the center and HI at the periphery. It shows, like CO, a central peak and an inner ring and, like HI, a weaker, extended plateau. This is the first time that dust emission is unambiguously

detected in extragalactic HI clouds. Like HI, the 1.2 mm contours are warped near the NW edge of the galaxy. The warp, already apparent at half the optical radius, reaches a height of 50″ (2.4 kpc) at the edge of the optical disk (Fig. 9).

The average dust temperature is 18 K near the center and 15 K in the HI plateau. From the 1.2 mm continuum intensity and the HI line integrated intensity, we derive a dust absorption cross section per H atom $\sigma^{\rm H}_{1.2\rm mm} = \tau/N_{\rm H} = 5 \times 10^{-27}$ cm^2 in the plateau. This value is very close to that predicted by Draine & Lee (1984) for the local diffuse clouds.

The velocity field derived from CO can be described by rotation (solid body rotation between 0 and 4 kpc, constant velocity further out) plus non-circular motions. The non-circular motions are observed mostly near the 'arms' and near the nucleus. They are are probably the signature of a spiral density wave and/or of a central bar. The presence of a bar could explain the boxy shape of the central bulge on optical photographs.

CO in the Barred Galaxy NGC 1530

D. Downes([1]), D. Reynaud([1]), P. M. Solomon([2]), S. J. E. Radford([3])
([1])Institut de Radio Astronomie Millimétrique, 38406 St. Martin d'Hères, France
([2])Astronomy Program, State University of New York, Stony Brook, NY 11794
([3])National Radio Astronomy Observatory, Tucson AZ 85721-0665

Abstract: We present observations of the barred spiral NGC 1530 in CO(1–0) with the IRAM Interferometer and in CO(1-0) and (2-1) with the IRAM 30 m telescope. Along the bar there is abundant molecular gas associated with the dust lanes seen on optical images. Near the nucleus, the interferometer maps show strong shock fronts and a nuclear ring. *There appears to be very little or no gas at the nucleus itself.* Perpendicular to the bar, the shock fronts are barely resolved and extend < 3″. Most of the molecular gas in the galaxy is in a central ellipse with a major axis of 3.5 kpc. This major axis and the strongest velocity gradients are *perpendicular* to the bar. Position-velocity diagrams are consistent with the molecular gas following elliptical orbits along the bar, but show important deviations at the strong shock fronts and close to the nucleus, where the gas follows orbits perpendicular to the bar. We also detect giant molecular complexes near the ends of the bar and much fainter CO in molecular clouds in the SE spiral arm. In spite of its high CO luminosity and great central concentration of molecular gas, the galaxy has only a modest $L_{\rm FIR}/L_{\rm CO}$ ratio, which suggests a relatively low rate of star formation. Although the molecular gas has a latent capacity to fuel a large starburst, further infall to the center is probably hindered by the closed orbits 1.5 kpc from the nucleus. Hence most of the gas cannot attain the critical density needed for a large starburst.

New observations and a new interpretation of CO(3-2) in IRAS F 10214+4724

D. Downes([1]), P. M. Solomon([2]), S. J. E. Radford([3])
([1])Institut de Radio Astronomie Millimétrique, 38406 St. Martin d'Hères, France
([2])Astronomy Program, State University of New York, Stony Brook, NY 11794
([3])National Radio Astronomy Observatory, Tucson AZ 85721-0665

Abstract: New observations with the IRAM interferometer of CO(3-2) from the highly luminous galaxy IRAS F 10214+4724 show the source is $1.5'' \times \leq 0.9''$; they display no evidence of any velocity gradient. This size, together with optical and IR data that show the galaxy is probably gravitationally lensed, lead to a new model for the CO distribution. In contrast to many lensed objects, we have a good estimate of the intrinsic CO and far IR surface brightnesses, so we can derive the CO and far IR/sub-mm magnifications. The CO is magnified 10 times and has a true radius of 400 pc and the far IR is magnified 13 times and has a radius of 250 pc. The true far IR luminosity is $4-7 \times 10^{12}$M$_\odot$ and the molecular gas mass is 2×10^{10}M$_\odot$. This is nearly an order of magnitude less than previously estimated. Because the far IR magnification is lower than the mid and near IR magnification, the intrinsic spectral energy distribution now peaks in the far infrared. That is, nearly all of the energy of this object is absorbed and re-emitted in the far infrared. In CO luminosity, molecular gas content, CO linewidth, and corrected far IR luminosity, 10214+4724 is a typical, warm, IR ultraluminous galaxy.

First millimeter mapping of the jet and nucleus of M87

V. Despringre([1]), D. Fraix-Burnet([1]), E. Davoust([2])
([1])Laboratoire d'Astrophysique de Grenoble, BP 53X, F-38041 Grenoble Cédex, France
([2])Laboratoire d'Astrophysique, Observatoire Midi-Pyrénées, 14 Avenue Edouard Belin, 31400 Toulouse, France

Abstract: Observations of M87 at 89 GHz (3.4 mm) with the IRAM Plateau de Bure interferometer are presented. This is the first image of an extragalactic jet at this frequency with such a resolution ($2.9'' \times 1.8''$). Knots A, B, C and G in the jet are clearly seen. The photometry of the knots reveals that, within the error bars, the millimetric intensity is that expected from a linear interpolation between the radio and optical values. An extended feature

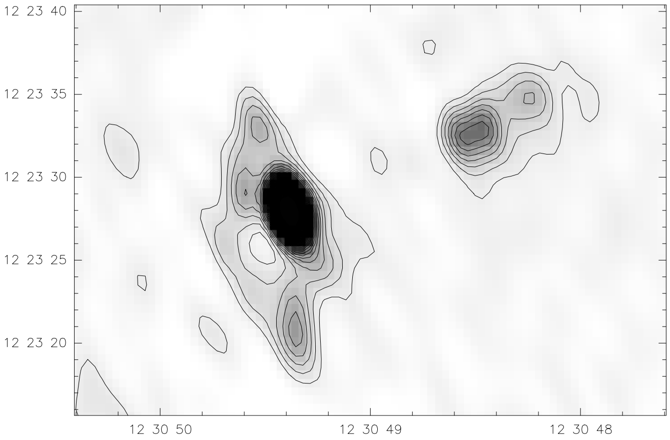

Figure 10: Grey map of M87 with contour level spacing of 35 mJy/beam and a peak intensity of 1.67 Jy/beam. The beamwidth is $2.9'' \times 1.8''$ at PA=22°.

of about $13'' \times 7''$ appears around the nucleus, which we were not able to attribute to an artifact. It is elongated perpendicular to the jet and its offset from the nucleus is symmetric to that of the well known H_α emission-line features in M87. If interpreted as very cold gas ($T \lesssim 10$ K), this extended structure would then have a total mass of $\simeq 10^{12}$ $M_\odot$.
Astronomy & Astrophysics, in press

80 - 360 GHz VERY WIDE BAND MILLIMETER WAVE NETWORK ANALYZER

F. Mattiocco, M.Carter
Institut de Radio Astronomie Millimétrique, 38406 St. Martin d'Hères, France

Abstract: Millimeter receivers made for the Radio Astronomy use devices and materials whose transmission, and reflection properties have to be known over a 40% bandwidth. We have made a millimeter extension to an HP8510C vector analyzer, which at present allows magnitude and phase measurement between 80 and 360 GHz with a sensitivity of ±0.2 dB and ±1 deg rms respectively over 30% instantaneous bandwidth for the transmission, and 23% for the reflection. Improvements relative to the first version include new harmonic mixers, and an active doubler. Dynamic ranges up to 60 dB in transmission and 50 dB in reflection are obtained up to 280 GHz, with more than 50 GHz instantaneous bandwidth using waveguide calibration. Detection with a 30 dB dynamic range is obtained at 320−360 GHz. Time domain measurements give spatial resolution down to 2 mm.
To appear in: Digest of the 20th Int. Conf. on Infrared and Millimeter Waves, Florida, USA, Dec. 1995.

New Preprints

The following preprints are available from IRAM:

365. millimeter-wavelength observations of compact steep-spectrum sources
H. Steppe, S. Jeyakumar, D.J. Saikia, C.J. Salter
1995 *Astron. and Astrophys.*

366. The Plateau de Bure survey of galactic λ3mm HCO^+ absorption toward compact extragalactic continuum sources
R. Lucas and H.S. Liszt
1995 *Astron. and Astrophys.*

367. Millimeter-wave absorption studies of the onset of dark-cloud chemistry
R. Lucas and H.S. Liszt
1995 *Communication presented in Tucson (May 1995)*
'CO 25 Years of Millimeter Wave Spectroscopy'

368. A precessing jet in the l1157 molecular outflow
F. Gueth, S. Guilloteau, R. Bachiller
1995 *Astron. and Astrophys.*

369. A search for CO emission in high redshift powerful radio galaxies
A.S. Evans, D.B. Sanders, J.M. Mazzarella, P.M. Solomon, D. Downes, C. Kramer, S.J.E. Radford
1995 *Astrophys. Journal*

370. Search for CO emission in globular clusters S. Leon and F. Combes
1995 *Astron. and Astrophys.*

371. Search for interstellar Glycine
F. Combes, Nguyen-Q-Rieu, G. Wlodarczak
1995 *Astron. and Astrophys.*

372. First millimeter mapping of the jet and nucleus of M87
V. Despringre, D. Fraix-Burnet, E. Davoust
1995 *Astron. and Astrophys.*

373. CO in the barred galaxy NGC 1530
D. Downes, D. Reynaud, P.M. Solomon, S.J.E. Radford
1995 *Astrophys. Journal*

374. Dust and gas distribution around T Tauri stars in Taurus-Auriga: I. Interferometric 2.7 mm continuum and ^{13}CO J=1-0 observations
A. Dutrey, S. Guilloteau, G. Duvert, L. Prato, M. Simon, K. Schuster, E. Ménard
1995 *Astron. and Astrophys.*

375. High resolution radio continuum polarization of M51
N. Neininger, C. Horellou
1995, Proc. of the Conference on Polarimetry of the Interstellar Medium, Troy, NY

376. Cold dust and molecular line emission in NGC 4565
N. Neininger, M. Guélin, S. Garcia-Burillo, R. Zylka, R. Wielebinski
1995 *Astron. and Astrophys.*

377. The 30-m Manual: A Handbook for the IRAM 30-m Telescope (Version 1.0)
W. Wild
1995, October 27

378. The molecular envelope around 89 HER
J. Alcolea, V. Bujarrabal
1995 *Astron. and Astrophys.*

379. Water emission at 183 GHz from HH 7-11 and other low-mass star-forming regions
J. Cernicharo, R. Bachiller, E. Gonzalez-Alfonso
1995 *Astron. and Astrophys.*

Programmes scheduled on the 30-m telescope in 1995

JAN 3 - 17

Ident.	Title	Freq. (GHz)	Authors
219.94	Search for LiH rotational lines in collapsing primordial clouds at high redshifts	97, 145, 217	Maoli, de Bernardis, Melchiorri, Encrenaz, Signore
206.94	First chemical study of circumstellar disks	88, 113, 226, 260, 267	Dutrey, Guilloteau, Guélin
237.94	Outflow from the most symmetric protostellar jet : HH212	230,132	McCaughrean, Zinnecker, Gueth, Dutrey, Guilloteau
105.94	Search for hydrogeneous compounds in the Martian atmosphere	115, 251, 236	Rosenqvist, Marten, Moreau, Moreno
107.94	Observation of Titan in the (3-2) line of HCN and detection of the ^{12} C/^{13}C ratio from ^{13}CO and H^{13}CN lines	115, 220, 259	Marten, Hidayat, Bézard, Paubert
188.94	The spatial extent and abundance of water vapor in molecular clouds	183, 86, 230, 80, 204, 143	Cernicharo, Gonzalez, Bachiller
222.94	Pumping ^{29}SiO and ^{29}SiO maser emission through infrared line overlaps	85, 128, 171, 214, 257	Gonzalez, Cernicharo
173.94	Methanol abundance enhancement around young stellar objects	96, 109, 141, 219, 241	Bachiller, Colomer, Liechti, Walmsley

JAN 17 - 31

Ident.	Title	Freq. (GHz)	Authors
195.94	CO excitation and H_2 masses of IR luminous galaxies : a proposal to observe the CO(3-2) line	339, 331, 316	Solomon, Downes, Greve
129.94	Probing the different molecular gas components in the nucleus of IC342	265, 259, 241, 354	Schulz, Guesten
147.94	High angular resolution of IRC+10216 : a key to the understanding of chemical processes in circumstellar envelopes	110, 113	Lucas, Guélin, Cernicharo, Kahane
138.94	2mm DCO+ absorption toward extragalactic continuum sources	144	Liszt, Lucas
145.94	Vibrationally excited CS in star forming cores	96, 241, 337, 340	Hauschildt, Guesten
197.94	CO+ in photon dominated regions	89, 235, 267, 354	Stoerzer, Sternberg, Stutzki
109.94	Mass-loss in carbon Miras with small pulsation periods	115, 230, 345	Groenewegen, Omont
134.94	A beta-line maser in MWC349 ?	335, 366, 353	Thum, Martin-Pintado, Strelnitski
176.94	HCN (3-2) and (4-3) in ultraluminous IR galaxies	85, 254,3 39, 86, 261	Gao, Solomon, Downes, Radford

Jan 31 - Feb 14

Ident.	Title	Freq. (GHz)	Authors
233.94	The mm continuum emission from QSO's with z>4	Bolometer	Omont, McMahon, Bergeron, Cox, Kreysa
114.94	Search for cold dust envelopes around Herbig Ae/Be stars	Bolometer	Henning, Leinert, Fiebig
115.94	The youngest stellar cores in Bok globules - 1.3mm continuum mapping	Bolometer	Launhardt, Henning, Zylka
214.94	Mm continuum emission from radio weak quasars	Bolometer	MacMahon, Omont
209.94	Cold dust in NGC891, M51 and IC342 : a key to the molecular gas content of spiral galaxies	Bolometer	Zylka, Guélin, Mezger, Haslam, Kreysa, Sievers, Garcia-Burillo
122.94	An investigation of B3-VLA sources at λ1.3mm	Bolometer	Klein, Vigotti, Fanti, Gregorini, Reuter, Mack
142.94	Multichannel bolometer observations of 2060 Chiron near Perihelion	Bolometer	Altenhoff, Stern, Weintraub, Festou

Feb 14 - Feb 28

Ident.	Title	Freq. (GHz)	Authors
122.94	An investigation of B3-VLA sources at λ1.3mm	Bolometer	Klein, Vigotti, Fanti, Gregorini, Reuter, Mack
142.94	Multichannel bolometer observations of 2060 Chiron near Perihelion	Bolometer	Altenhoff, Stern, Weintraub, Festou
225.94	Simultaneous mm/gamma-ray observations of bright BL Lac objects	Bolometer	Wagner, Witzel, Krichbaum
162.94	Dust at high redshift : are QSOs and luminous IR galaxies related ?	Bolometer	Ivison, Chini, Seaquist, Papadopoulos
143.94	The first high-resolution maps of the Cas A and Crab SNRs at 1.3mm	Bolometer	Holland, Greaves
248.94	Cold dust around high redshift quasars	Bolometer	Andreani, Casoli, Gerin, Cristiani, Lafranca
187.94	Cold circumstellar dust around newly ROSAT discovered T Tauri stars	230	Bouvier, André
163.94	Continuum observations of symbiotic stars : testing the standard model	Bolometer	Ivison, Seaquist
199.94	Structure of pre-protostellar cores	98, 147, 244, 342, 96, 144	André, Ward-Thompson, Motte
158.94	Deep 1.3mm observations of an X-ray selected complete sample of BL Lacertae objects	Bolometer	Gear

Feb 28 - Mar 14

Ident.	Title	Freq. (GHz)	Authors
	VLBI Observations and MPIfR Guaranteed Time		

MAR 14 - MAR 28

Ident.	Title	Freq. (GHz)	Authors
198.94	Size and density structure of low-mass protostellar envelopes	230	André, Motte, Neri
242.94	Completing the observations of the λ1.3mm emission in the edge- on galaxy NGC4565	Bolometer	Neininger, Zylka, Guélin, Dumke, Wielebinski
210.94	Cold dust in four giant cloud associations of M33	Bolometer	Guélin, Viallefond, Neininger, Zylka, Mezger
209.94	Cold dust in NGC891, M51 and IC342 : a key to the molecular gas content of spiral galaxies	Bolometer	Zylka, Guélin, Mezger, Haslam, Kreysa, Sievers, Garcia-Burillo
132.94	Dust properties in the isolated flocculent Sc galaxy NGC4414	Bolometer	Hoernes, Braine, Kruegel
119.94	Millimeter continuum emission in TMC-1	Bolometer	Cernicharo, Cox, André, Ward-Thompson, Zylka

MAR 28 - APR 11

Ident.	Title	Freq. (GHz)	Authors
210.94	Cold dust in four giant cloud associations of M33	115,230	Guélin, Viallefond, Neininger, Zylka, Mezger
165.94	The interstellar medium of nearby galaxies	Bolometer	Braine, Wielebinski, Guélin, Sievers
172.94	Extremely high-velocity CO emission in HH90/91	110, 115, 147, 230	Bachiller, Eisloeffel, Cernicharo
149.94	Detection of CO in galactic globular clusters	115, 230	Leon, Combes
128.94	Molecular clouds in the outer parts of galaxies : N891	115, 110, 230, 220	Combes, Garcia-Burillo, Casoli
229.94	Molecular absorption : a detailed study of the dense ISM at z=0.25 and z=0.68	87, 92, 115, 139, 145	Wiklind, Combes

APR 11 - APR 25

Ident.	Title	Freq. (GHz)	Authors
229.94	Molecular absorption : a detailed study of the dense ISM at z=0.25 and z=0.68	87, 92, 115, 139, 145	Wiklind, Combes
110.94	Molecular clouds in the prototype peanut galaxy NGC128	113, 227	Combes, Emsellem
191.94	Molecular line observations of high mass star forming GMC cores	96, 110, 144, 147	Mooney, Mauersberger, Mezger, Zylka
223.94	CO observations high redshift IRAS quasars	90, 96,108, 144, 161	Roettgering, Van Breugel, Lehnert
224.94	Neutral carbon in IRAS 10214+4724	197, 149, 246	Radford, Downes
246.94	Searching and mapping the outflows around selected T Tauri stars	97, 110, 144, 220	Menard, Lefloch, Plazy, Monin

APR 25 - MAY 9

Ident.	Title	Freq. (GHz)	Authors
226.94	The molecular content of prototypical molecular clouds	82, 115, 163, 204, 237	Cernicharo, Guélin, Kahane, Gonzalez
175.94	Disk temperature of the planets at 150 and 230GHz	150, 230	Greve, lefloch, Kramer, Moreno
146.94	CN and HCN in carbon rich circumstellar envelopes	88, 113, 226, 266	Lindqvist, Eriksson, Gustafsson, Lucas, Olofsson, Omont
160.94	A gravitational telescope to probe the gas content of distant normal galaxies	106, 108, 133, 142	Casoli, Fort, Boissé, Encrenaz, Mellier
221.94	CO observations of a sample of high redshift radio galaxies	103, 110, 138, 147, 153	Van Ojik, van der Werf, Miley, Roettgering
156.94	High density gas in megamaser galaxies	87, 84, 88	Baudry, Rieu, Baan, Henkel
172.94	Extremely heigh velocity CO emission in HH90/91	110, 115, 130, 220, 230	Bachiller, Eisloeffel, Cernicharo

MAY 9 - MAY 23

Ident.	Title	Freq. (GHz)	Authors
172.94	Extremely heigh velocity CO emission in HH90/91	110, 115, 130, 220, 230	Bachiller, Eisloeffel, Cernicharo
227.94	A systematic search for infall evidence in the youngest nearby stellar objects	98, 110, 145, 230	Bachiller, Tafalla, Myers, Mardones
170.94	Disruption of a dense core by an outflow in L1228 ?	115, 110, 147, 220	Tafalla, Myers, Bachiller, Chen, Wilner
120.94	CS towards the young stellar object NGC 2264-IRS1	97, 146, 219	Henning, Martin, van Dishoeck, Helmich
216.94	Circumstellar matter around Herbig Ae/Be stars	97, 183, 230	Fiebig, Papkalla, Launhardt
250.94	Molecular gas temperature, optical depth, and the N(H2)/lCO(1-0) factor. I : Isolated galaxies	109, 115, 219, 230	Braine, Brouillet, Baudry, Wielebinski
16.95	New molecular line observations of the cloverleaf quasar	92, 129, 161, 227	Barvainis, Alloin, Antonucci, Maloney
136.94	Search for CH_3OH on Titan	241	Bézard, Marten, Paubert
125.94	HCO^+ 1-0 emission toward a sample of young stellar objects in Taurus	89, 130, 219, 86	Van Dishoeck, Hogerheijde

MAY 23 - JUN 6

Ident.	Title	Freq. (GHz)	Authors
16.95	New molecular line observations of the cloverleaf quasar	92, 129, 161, 227	Barvainis, Alloin, Antonucci, Maloney
136.94	Search for CH_3OH on Titan	241	Bézard, Marten, Paubert
135.94	Pulsar detection at short mm wavelengths	80, 250	Morris, Thum, Booth
4.95	Confirming the detection of true low-mass protostars	96, 144, 115, 230	Guesten, Wiesemeyer, Fiebig
18.95	Anatomy of a dense core in the galactic cirrus	97, 99, 146, 219	Heithausen, Corneliussen, Grossmann
36.95	H_2S and N_2H^+ in the galactic cirrus	93, 168, 219	Grossmann, Corneliussen, Heithausen
31.95	SO_2, SO and OCS in the atmosphere of Io	221, 218, 143, 104	Lellouch, Strobel, Belton, Encrenaz, Gulkis, de Pater, Paubert
51.95	CO(2-1) observations along the anomalous Hα and radio arms of NGC 4258	230, 115, 88, 146	Cox, Downes

The IRAM Newsletter is edited by Robert LUCAS at IRAM-Grenoble (e-mail address: `lucas@iram.fr`).
The IRAM Newsletter is available in electronic form:

- by using the World Wide Web and NCSA Mosaic: from the IRAM home page (`http://iram.fr/`), click on item "Newsletter" and follow the links...
- by means of an anonymous `ftp` account, opened at IRAM for Internet users. To access those files, please connect through `ftp` to `iram.fr` (or `193.48.252.22`) and read the `README` file. Several subdirectories are available:

Directory	Contents
`/dist/newsletter`	Recent issues of this Newsletter (one subdirectory per issue)
e.g. `/dist/newsletter/jul95`	jul95.ps is the Postscript file for the July 1995 issue.
`/dist/doc`	Documentation on IRAM telescopes and software
`/dist/proposal`	Proposal forms and Latex files to aid proposal preparation
`/dist/soft`	distribution files for reduction software

- by means of an electronic mail file server installed at IRAM (on the VAX machine IRAM04). This file server is a file distribution service that uses electronic mail facilities to deliver files. To communicate with it you should send a message to the electronic address:

  `newsserv@iram.grenet.fr`

  For instance, to obtain a copy of the May 1992 issue, just send the one line message:

  `SENDME MAY92.PS`

  to the above electronic address. You will receive later a mail message containing the IRAM Newsletter in Postscript code. Please discard all the e-mail header information with a text editor, and send the file to a Postscript laser printer.

  More information may be obtained by sending the one line message:

  `HELP`

  Note that this file server also contains Postscript files of the proposal forms and of Plateau de Bure documentation.

We also compile a list of e-mail addresses of IRAM users (e.g., in order to send warning messages when the Newsletter is available, but also to provide fast information, if needed). If you feel your address should be on this list, please send the one line message:

`SUBSCRIBE`

to the following e-mail address:

`iramusers-request@iram.grenet.fr`

Both addresses are valid on Internet, EARN-Bitnet and EAN .... Please keep R. Lucas informed of any problem you may encounter.

IRAM Addresses:

	Address:	Telephone:	Fax:
Grenoble	Institut de Radioastronomie Millimétrique, 300 rue de la Piscine, Domaine Universitaire, 38406 St Martin d'Hères Cedex, France	(33) 76 82 49 00	(33) 76 51 59 38
Plateau de Bure	Institut de Radioastronomie Millimétrique, Observatoire du Plateau de Bure, 05250 St Etienne en Dévoluy, France	(33) 92 52 53 60	(33) 92 52 53 61
Granada	Instituto de Radioastronomía Milimétrica, Avenida Divina Pastora 7, Núcleo Central, 18012 Granada, España	(34) 58 22 88 99	(34) 58 22 23 63
Pico Veleta	Instituto de Radioastronomía Milimétrica, Estación Radioastronómica IRAM-IGN del Pico Veleta, Sierra Nevada, 18012 Granada, España	(34) 58 48 80 00	(34) 58 48 80 82

E-Mail Addresses:

- IRAM-Grenoble: `username@iram.fr`, or through PSI: `PSI%0208038080590::username`
- IRAM-Granada: `username@iram.es`, or through PSI: `PSI%02145258020628::username`

The `username` is generally the last name of the person to be contacted.